Nuclear Instruments and Methods in Physics Research B 286 (2012) 89–92

Contents lists available at SciVerse ScienceDirect

Nuclear Instruments and Methods in Physics Research B

journal homepage: www.elsevier.com/locate/nimb

Damage formation and recovery in Fe implanted 6H–SiC

P. Miranda [a], U. Wahl [a,b], N. Catarino [a], K. Lorenz [a,b], J.G. Correia [a,b], E. Alves [a,b,*]

[a] Instituto Tecnológico e Nuclear, EN10, 2696-953 Sacavém, Portugal
[b] Centro de Física Nuclear da Universidade de Lisboa, 1649-003 Lisboa, Portugal

ARTICLE INFO

Article history:
Received 12 August 2011
Received in revised form 13 October 2011
Available online 22 November 2011

Keywords:
6H–SiC
Ion implantation
Damage annealing
Lattice sites
Emission channeling

ABSTRACT

Silicon carbide doped with magnetic ions such as Fe, Mn, Ni or Co could make this wide band gap semiconductor part of the diluted magnetic semiconductor family. In this study, we report the implantation of 6H–SiC single crystals with magnetic $^{56}Fe^{+}$ ions with an energy of 150 keV. The samples were implanted with 5×10^{14} Fe^{+}/cm^{2} and 1×10^{16} Fe^{+}/cm^{2} at different temperatures to study the damage formation and lattice site location. The samples were subsequently annealed up to 1500 °C in vacuum in order to remove the implantation damage. The effect of the annealing was followed by Rutherford Backscattering/Channeling (RBS/C) measurements. The results show that samples implanted above the critical amorphization temperature reveal a high fraction of Fe incorporated into regular sites along the ⟨0001⟩ axis. After the annealing at 1000 °C, a maximum fraction of 75%, corresponding to a total of 3.8×10^{14} Fe^{+}/cm^{2}, was measured in regular sites along the ⟨0001⟩ axis.

A comparison is made between the observed annealing behavior and the one measured in low fluence (2×10^{13} cm^{-2}) β emission channeling experiments using the radioactive isotope ^{59}Fe ($t_{1/2}$ = 45 d), where the sample was implanted at room temperature and the β^{-} emission channeling yield was measured by means of a position-sensitive detector.

1. Introduction

The quest for diluted magnetic semiconductor (DMS) materials is among the most intensively researched areas worldwide [1,2]. The possibility to use spin polarization to create new functionalities for electronics and photonics makes this field interesting for the semiconductor industry. Triggered by its unique properties for high power devices, during the last decade a considerable amount of work was also performed on possible applications of silicon carbide in spintronics [3,4]. To achieve this goal there are three major issues to solve: the material must be a ferromagnetic semiconductor, the value of the Curie temperature must be around room temperature (or above) and the matrix must remain a dilute solution instead of forming metal clusters or second phases. The availability of different SiC polytypes opens a great number of possibilities depending on the structure of the polytype. The magnetic properties of SiC doped with transition metals have been studied theoretically, and the results, although controversial in some cases, suggest the dependence of the magnetism on the site occupation of the metallic ions [5,6]. The interpretations of the experimental results, on the other hand, are complicated by the formation of new phases or clustering of the impurities which could be the origin of the magnetic properties [7,8].

The low solubility of impurities in SiC poses a problem when we try to incorporate large amounts of magnetic dopants while keeping the structural integrity of the matrix. In any case, the need for a non-equilibrium technique like ion implantation is necessary to achieve the required concentrations. As a violent process, implantation creates damage and as a binary compound the defects in both sublattices (Si and C) raise a multitude of defect configurations that need to be annealed. The defect production and annealing of the different SiC polytypes was studied by several groups, and it is reasonably well understood [9–12]. The short range nature of the covalent bonds makes SiC very radiation sensitive and easy to amorphize, and temperatures above 1000 °C are necessary to promote defect recovery. The recrystallization and stability of the implanted species in the lattice are key issues for the integration of the implantation technique in the doping process of SiC for spintronic applications.

In this study we present results of Fe implantation in 6H–SiC at different temperatures and fluences. The damage formation and annealing was studied by Rutherford Backscattering/Channeling. The stability and lattice site location of the iron ions in the SiC structure was followed by emission channeling (EC) and detailed RBS/C angular scans through the ⟨0001⟩ direction.

2. Experimental details

6H–SiC single crystal samples were cut from a wafer obtained from CrysTec GmbH and implanted with Fe ions over the

* Corresponding author at: Instituto Tecnológico e Nuclear, EN10, 2696-953 Sacavém, Portugal. Tel.: +351 219946086.
E-mail address: ealves@itn.pt (E. Alves).

0168-583X/$ - see front matter © 2011 Elsevier B.V. All rights reserved.
doi:10.1016/j.nimb.2011.10.072

temperature range from 25 (RT) to 550 °C, with the beam tilted 10° off the *c*-axis, an energy of 150 keV and fluences of 5×10^{14} Fe^+/cm^2 and 1×10^{16} Fe^+/cm^2. According to SRIM [13], the Fe range is 83 nm, which is slightly higher than the experimental value, 75 nm. The control of the fluence was obtained by integration of the beam current, kept below 0.5 μA/cm^2 to avoid dose rate effects [14]. Some selected samples were further rapid thermal annealed (RTA) at 1000 °C and 1500 °C for 30 s at a pressure of 5×10^{-4} Pa. The crystalline quality and structural properties of the samples were characterized by RBS/C. A collimated 2 MeV He^+ beam delivered by a Van de Graaff accelerator was used as analyzing beam in order to determine the implantation and damage profiles of the samples. Channeling measurements were done along the ⟨0001⟩ axes to inspect the displaced atoms. The lattice site location of the Fe ions along the ⟨0001⟩ atomic rows was performed by detailed angular scans.

For the emission channeling experiments, the radioactive isotope ^{59}Fe ($t_{1/2}$ = 45 d) was produced and implanted at low fluence (2×10^{13} cm^{-2}) into a 6H–SiC single crystal with 60 keV 10° off the surface normal at CERN's ISOLDE facility. The angular-dependent count rate of the emitted β^- particles in the energy range 50–461 keV was then measured using a 3×3 cm^2 position-sensitive Si pad detector of 22×22 pixels placed at 29 cm from the sample.

3. Results and discussion

3.1. Structural analysis

The 6H–SiC single crystals are very radiation sensitive and became amorphous at very low implantation fluences. The predicted SRIM recoils and Fe profiles are displayed in Fig. 1. The Si and C recoil profiles nearly overlap despite the different mass and displacement energies used in the simulation, 20 eV for C and 35 eV for Si respectively [15]. The presence of C and Si displaced atoms at close distances favors the recrystallization process, despite the imbalance of the total number of recoils predicted by the SRIM results. At room temperature, the amorphous transformation is already observed for the lowest implanted fluence, 5×10^{14} Fe^+/cm^2, as indicated by the overlap of the random and aligned spectra through the entire implanted region (~150 nm) shown in Fig. 2. Damage accumulation in the SiC polytypes under irradiation has been explained

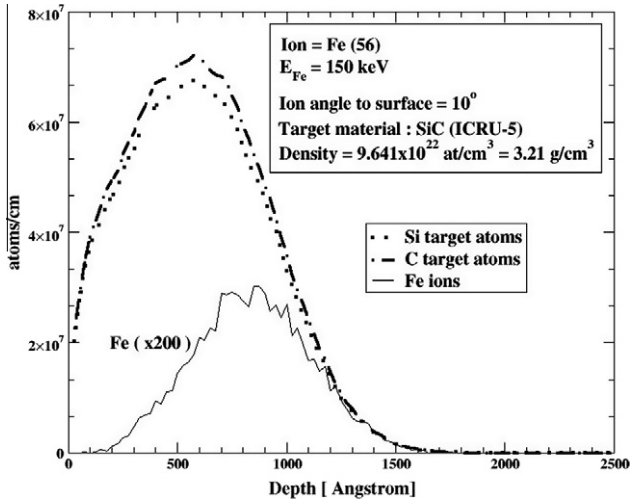

Fig. 1. Recoils and Fe implantation profile obtained with SRIM code. Despite the different mass and displacement energies, the recoil profiles differ only in the total number of C and Si recoils.

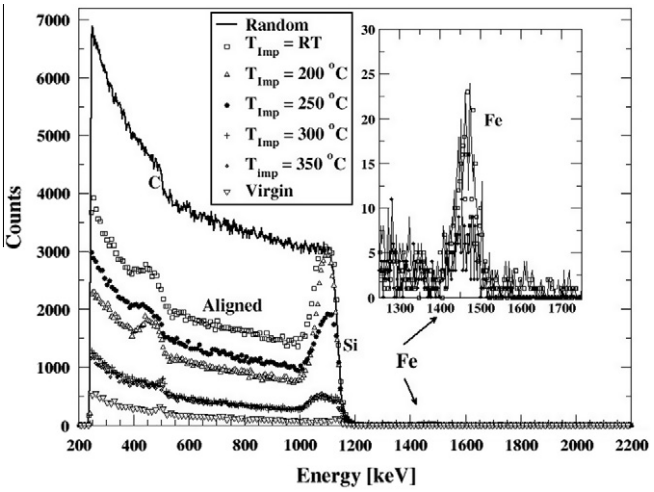

Fig. 2. Random and ⟨0001⟩ aligned RBS spectra from 6H–SiC implanted with a nominal fluence of 5×10^{14} Fe^+/cm^2 at different temperatures.

by several models based on the direct impact mechanism [16,17]. In the model proposed by Jagielski et al. [17] a multi step accumulation of the damage (MSDA) is considered. The model reproduces quite well the results obtained by Debelle et al. [12] for a 100 keV implantation, and an amorphization threshold of 0.45 dpa was established for 6H–SiC. Here, the displacements per atom are around 0.7 dpa, and the implanted region is rendered amorphous for all the implantations at RT. The increase of the implantation temperature promotes the annealing of the defects, inhibiting the amorphization. At 200 °C the width of the amorphous layer is reduced, and above 300 °C the samples remain crystalline with some residual damage distributed over the implanted region. The results are summarized in Fig. 3 where we plot the evolution of the difference of the minimum yield $\Delta\chi_{min}$ ($\Delta\chi_{min} = {}^{Imp}\chi_{min} - {}^{Vir}\chi_{min}$, the difference of minimum yields for the virgin and implanted samples at the same depth) with the temperature. From the curve, we could estimate a value of 250 °C for the critical temperature above which the amophization is prevented in SiC, which is very similar to the value (around 230 °C) found by Weber et al. [11]. We have implanted fluences as high as 1×10^{16} Fe^+/cm^2 at 350 °C and only a buried damage region developed at the depth of the implanted ions. The nature of the damage could not be determined with RBS/C, but other studies in similar conditions show the presence

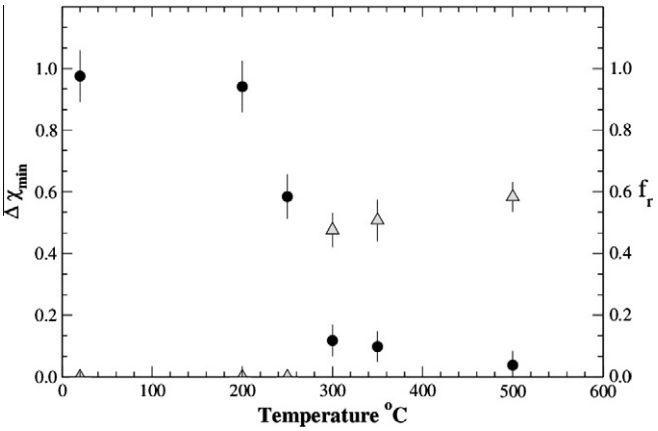

Fig. 3. Evolution of the damage (circles) with the implantation temperature in the Si sublattice at the implanted depth according to the results of Fig. 2. The regular fraction of Fe (triangles), f_r, is also shown on the right axis, as explained in the text.

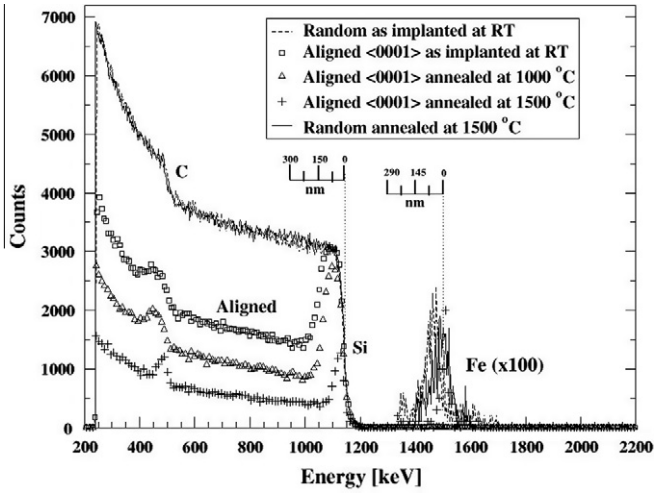

Fig. 4. Random and ⟨0001⟩ aligned spectra showing the recrystallization of the amorphous layer of the sample implanted at room temperature with 5×10^{14} Fe^+/cm^2. Despite the Fe redistribution the total amount was conserved.

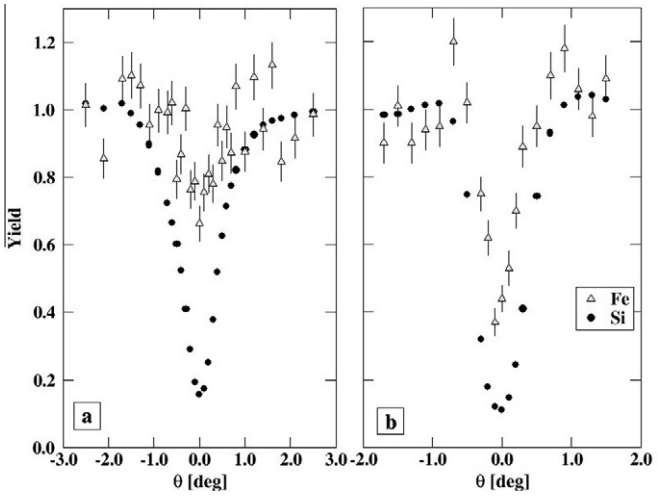

Fig. 5. Angular scan through the ⟨0001⟩ axis after implantation (a) and annealing at 1000 °C (b) for the samples implanted at 350 °C with 5×10^{14} Fe^+/cm^2.

of dislocations and localized amorphous zones in the implanted region [10,11]. Recently Wendler et al. [18] showed the presence of different mechanisms for defect annealing during the implantation above 200 °C. The mobility of point defects, vacancies mostly, play a major role in defect annihilation up to 350 °C in the low fluence implantation regime. For high fluences, the role of the implanted species must be considered, and we could not rule out the formation of other phases (iron silicides) during the implantation. In our study, the XRD results (not shown) did not reveal any evidence for the presence of other phases, but the interaction volume could not be sufficient to produce a measurable signal.

The recovery of the damage is an important step in all the implantation processes. The presence of different chemical species and defect concentrations makes the recrystallization process in SiC difficult. The evolution of the amorphous layer with annealing temperature is shown in Fig. 4. A layer by layer recrystallization starting at the amorphous/crystalline interface explains the decrease of the thickness of the original amorphous layer at 1000 °C. A value of 1.7 nm/s was estimated for the regrowth velocity at this temperature. The annealing at 1500 °C promotes the complete recrystallization of the amorphous layer. The higher value of the minimum yield after the annealing is due to some residual damage at the surface that gives rise to the C and Si surface peaks observed in the aligned spectrum. What is more surprising is the retention of the implanted Fe in the crystal. In the literature, different groups reported that at this high temperature the implanted species outdiffuse and are lost through the surface [10,19]. Our results show the redistribution of the Fe, but a significant fraction is incorporated into the recrystallized lattice suggesting the possibility to achieve the full activation of the Fe ions in 6H–SiC.

3.2. Site location

An important aspect of the incorporation of impurities in materials is the site location. The comparison of the random and aligned yield of Fe indicates the incorporation of a large fraction into regular sites. The maximum regular fraction f_r of Fe($f_r = 1 - {}^{Fe}\chi_{min}/1 - {}^{Si}\chi_{min}$) introduced in lattice sites along the ⟨0001⟩ axis during the implantation was 60%, which was obtained for the sample implanted at 500 °C. To obtain a more precise information about the position of the Fe ions, we performed detailed angular scan through the ⟨0001⟩ direction. The results obtained after the implantation and annealing at 1000 °C for the sample implanted with 5×10^{14} Fe^+/cm^2 are shown in Fig. 5. The regular fraction increases from 45% to about 75%. However, it is evident that the Fe curve is narrower than the Si, which is an indication that the ions were not occupying a pure substitutional site in the Si sublattice.

In addition, we obtained first results with very low fluences of implanted Fe by means of β^- emission channeling from radioactive ^{59}Fe, where the influence of the implantation damage is very small. For that purpose 2×10^{13} cm^{-2} of 60 keV ^{59}Fe ions was implanted with 60 keV at room temperature, and the β^- emission yield measured around the major crystallographic directions by means of a position-sensitive detector [20]. Fig. 6 shows the emission channeling pattern along the *c*-axis in the as-implanted state. The clear channeling effects of the axial ⟨0001⟩ and the family of planar (11–20) directions show that a considerable fraction of the Fe probes are located in sites that are aligned with the mixed rows of Si and C atoms. A preliminary analysis by means of comparing to many-beam simulations of electron emission channeling gave two interesting results. First, the absence of electron channeling effects along the family of (−1100) planes for substitutional emitter atoms seems to be a characteristic of the 6H structure; second, the

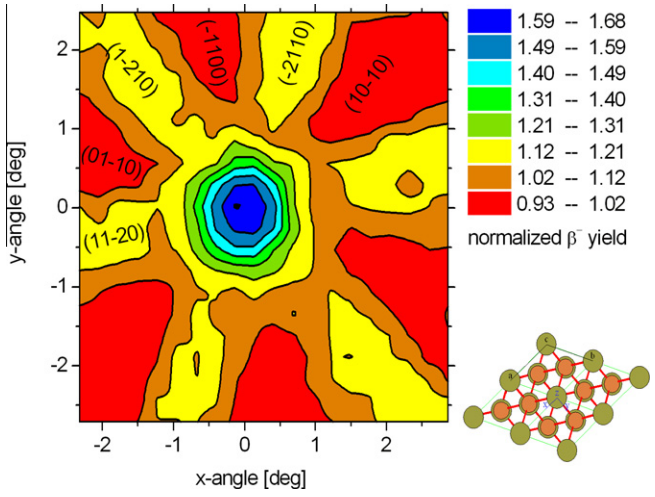

Fig. 6. Normalized β^- emission yield around the ⟨0001⟩ direction of a ^{59}Fe implanted 6H–SiC crystal. The inset in the lower right hand corner shows the orientation of the crystal during the measurement.

pattern is well compatible with a significant fraction of emitter atoms being located on interstitial sites displaced from the *c*-axis.

To obtain a precise lattice site location of the Fe ions in the 6H–SiC structure we need to perform more detailed RBS/C angular scans through tilted axial directions and compare all data to the results of Monte Carlo simulations. Similarly, for the emission channeling experiments the patterns need to be fully analyzed by fitting to the results of many-beam simulations. Due to the large number of available sites in the lattice, this is a complex task and the results will be published in an independent paper.

4. Conclusions

The introduction of Fe ions into 6H–SiC regular lattice sites using ion implantation was successfully achieved. The amorphization is avoided by implanting at temperatures above 250 °C. For the samples implanted at lower temperatures, the amorphous layer regrows epitaxially at 1500 °C. The recrystallization induces the redistribution of the Fe ions in the implanted region with some segregation towards the surface, but the total amount of Fe is conserved. The samples implanted above the critical amorphization temperature show a high fraction of Fe incorporated into regular sites along the ⟨0001⟩ axis. After the annealing at 1000 °C, a maximum fraction of 75%, corresponding to a total of 3.8×10^{14} Fe^{+}/cm^{2}, was measured in regular sites along the ⟨0001⟩ axis.

Acknowledgements

We acknowledge financial support from the Portuguese Foundation for Science and Technology through CERN/FP/116320/2010 and PTDC/CTM/100756/2008 as well as the SPIRIT project, EC Grant agreement No. 227012-CP-CSA-Intra. The authors also thank the assistance of S. Miranda during the RTA and J. Rocha for the implantations.

References

[1] S.J. Pearton, C. R Abernathy, D.P. Norton, A.F. Hebard, Y.D. Park, L.A. Boatner, J.D. Budai, Mater. Science Eng. R40 (2003) 37–168.
[2] T. Dietl, H. Ohno, F. Matsukara, J. Cibert, D. Ferrand, Science 287 (2000) 1019.
[3] N. Theodoropoulou, A.F. Hebard, S.N.G. Chu, M.E. Overberg, C.R. Abernathy, S.J. Pearton, R.G. Wilson, J.M. Zavada, Y.D. Park, J. Vac. Sci. Tech. A 20 (2002) 579.
[4] H. Pan, Y.W. Zhang, V. Shenoy, H. Gao, Appl. Phys. Lett. 96 (2010) 192510.
[5] M.S. Miao, W.R.L. Lambrecht, Phys. Rev. B 68 (2003) 125204.
[6] A. Los, V. Los, J. Phys.: Condens. Matter 21 (2009) 206004.
[7] F. Takano, W. Wang, H. Akinaga, H. Ofuchi, S. Hishiki, T. Ohshima, J. Appl. Phys. 101 (2007) 09N510.
[8] C. Dupeyrat, A. Declémy, M. Drouet, D. Eyidi, L. Thomé, A. Debelle, M. Viret, F. Ott, Physica B 404 (2009) 4731–4734.
[9] W.J. Weber, W. Jiang, F. Gao, R. Devanathan, Nucl. Instrum. Meth. B 190 (2002) 261–265.
[10] E. Wendler, A. Heft, W. Wesch, Nucl. Instrum. Meth. B 141 (1998) 105–117.
[11] W.J. Weber, L.M. Wang, N. Yu, N.J. Hess, Mat. Science and Eng. A253 (1998) 62–70.
[12] A. Debelle, L. Thomé, D. Dompoint, A. Boulle, F. Garrido, J. Jagielski, D. Chaussende, J. Phys. D: Appl. Phys. 43 (2010) 455408.
[13] J. F. Ziegler, J. P. Biersack, U. Littmark, The stopping and ranges of ions in matter, Pergamon Press, New York, 2003; www.srim.org.
[14] Y. Zhang, W.J. Weber, W. Jiang, C.M. Wang, A. Hallen, G. Possnert, J. Appl. Phys. 93 (2003) 1954–1960.
[15] R. Devanathan, W.J. Weber, F. Gao, J. Appl. Phys. 90 (2001) 2303.
[16] W.J. Weber, Nucl. Instrum. Meth. B166–167 (2000) 98.
[17] J. Jagielski, L. Thomé, Appl. Phys. A: Mat. Sci. Process 97 (2009) 147.
[18] E. Wendler, Th. Bierschenk, W. Wesch, E. Friedland, J.B. Malherbe, Nucl. Instrum. Meth. B 268 (2010) 2996–3000.
[19] A. Kozanecki, C. Jeynes, B.J. Sealy, A. Nejim, Nucl. Instrum. Meth. B136–138 (1998) 1272–1276.
[20] U. Wahl, J.G. Correia, A. Czermak, S.G. Jahn, P. Jalocha, J.G. Marques, A. Rudge, F. Schopper, J.C. Soares, A. Vantomme, P. Weilhammer, The ISOLDE collaboration, Nucl. Instr. Meth. A 524 (2004) 245.